ENVIRONMENTAL RESEARCH
LETTERS

LETTER • OPEN ACCESS

Terrestrial moisture sources dominate summer precipitation fluctuations in Northwest China

To cite this article: Peng Qian *et al* 2024 *Environ. Res. Lett.* **19** 124052

ENVIRONMENTAL RESEARCH
LETTERS

LETTER

Terrestrial moisture sources dominate summer precipitation fluctuations in Northwest China

Peng Qian[1], **Bin Zhu**[1,*], **Tong Zhu**[2], **Chenwei Fang**[1], **Chunsong Lu**[1], **Haishan Chen**[3] and **Hong Liao**[4]

[1] Collaborative Innovation Centre on Forecast and Evaluation of Meteorological Disasters, Key Laboratory for Aerosol-Cloud-Precipitation of China Meteorological Administration, Key Laboratory of Meteorological Disaster, Ministry of Education (KLME), Special test field of National Integrated meteorological observation, Nanjing University of Information Science and Technology, Nanjing, People's Republic of China
[2] IMSG at NOAA, NESDIS/STAR, 5830 University Research Ct., College Park, MD, United States of America
[3] Key Laboratory of Meteorological Disaster, Ministry of Education/International Joint Research Laboratory on Climate and Environment Change/Collaborative Innovation Center on Forecast and Evaluation of Meteorological Disasters, and School of Atmospheric Sciences, Nanjing University of Information Science and Technology, NUIST–University of Readin International Research Institute, Nanjing, People's Republic of China
[4] Jiangsu Key Laboratory of Atmospheric Environment Monitoring and Pollution Control, Jiangsu Collaborative Innovation Center of Atmospheric Environment and Equipment Technology, Joint International Research Laboratory of Climate and Environment Change, School of Environmental Science and Engineering, Nanjing University of Information Science and Technology, Nanjing, People's Republic of China
[*] Author to whom any correspondence should be addressed.

E-mail: binzhu@nuist.edu.cn

Keywords: Northwest China, atmospheric water tracer, precipitation fluctuations, terrestrial moisture sources

Supplementary material for this article is available online

OPEN ACCESS

RECEIVED
14 August 2024

REVISED
14 October 2024

ACCEPTED FOR PUBLICATION
25 October 2024

PUBLISHED
15 November 2024

Abstract

Northwest China (NWC), is characterized by its arid and semi-arid environment, and exhibits high sensitivity to precipitation variations. Recent research indicates a wetting tendency over NWC, yet quantifying its moisture source remains challenging. Here, employing a 40 year simulation with Community Atmosphere Model version 5.1 (CAM5.1) coupled to an atmospheric water tracer algorithm, we ascertain that the dominant source of summer moisture over NWC are from terrestrial sources (82% of vapor and 77% of precipitation), i.e. from local evaporation, North Asia (NA), Europe (EUP), the southern Tibetan Plateau (STP), and southeastern China (SEC), rather than oceanic sources. Favorable synoptic patterns over NWC enhance the precipitation-conversion efficiency from the southeasterly airflow transport (STP and SEC) compared to northwesterly airflow (NA and EUP). We also find that the fluctuations in precipitation over NWC, manifesting as alternating dry and wet summers, are primarily driven by increased moisture contributions from direct inputs from NA and re-evaporation transport from STP. Our study indicates that moisture variability in inland is predominantly driven by nearby terrestrial sources and underscores the complex mechanisms of terrestrial moisture transport.

1. Introduction

Northwest China (NWC, encompassing the provinces of Shaanxi, Gansu, Qinghai, Ningxia, and Xinjiang across approximately 3.12 million square kilometers) lies in the Eurasia hinterland and covers 85% of China's arid or semi-arid land area. The region is characterized by a dry climate, sparse vegetation, and a fragile ecological environment (Zhang *et al* 2000, Qian *et al* 2007, Li *et al* 2016, Gao *et al* 2018). However, in recent decades, global warming (0.13 °C decade^{-1}) has accelerated temperature increases in NWC (0.33 °C decade^{-1}), accompanied by a statistically significant rise in precipitation (5.5 mm decade^{-1}, Shi *et al* 2003, Li *et al* 2012, Deng *et al* 2022). Consequently, the NWC has undergone a warming-wetting climate shift, increasingly affecting both socio-economic dynamics (Peng *et al* 2017) and the ecological balance (Zhang *et al* 2021) in the region. The combination

of increased precipitation and rising temperatures has also reshaped local hydrological cycles and vulnerable ecosystems, intensifying occurrences of extreme precipitation events (Li *et al* 2021, Lu *et al* 2021, Wang *et al* 2022, Zhang *et al* 2022) previously uncommon.

Increased precipitation in NWC primarily results from local evapotranspiration and external advection, with external transport predominating (Wu *et al* 2019). For instance, interdecadal warming of the North Atlantic and Indo-Pacific warm pools has intensified northeasterly water vapor transport from the North Pacific, significantly boosting precipitation in NWC (Wu *et al* 2022). The eastward shift of the South Asian High has also redirected moisture from the upper westerlies and tropical Indian Ocean towards northwestern NWC (Wang *et al* 2005, Qu *et al* 2023). Some studies using Lagrangian trajectory methods (FLEXPART) have identified local evaporation and northwestern Asia as principal sources for western NWC (Xinjiang, Hu *et al* 2021). Additionally, hydrogen–oxygen isotope tracing has also pinpointed moisture over NWC originating from the southern continent of the EUP and NA (Zhang *et al* 2007, Bonne *et al* 2014). These studies have elucidated major moisture sources in NWC, while accurately quantifying these sources and understanding the transport mechanisms affecting precipitation variability remain challenging. The Eulerian atmospheric water tracer (AWT) method can accurately quantify the contributions from various moisture sources and reveals interannual and decadal atmospheric circulation patterns affecting terrestrial and oceanic moisture transport (Pan *et al* 2017, Jiang *et al* 2020). In this study, by integrating the AWT method with back-trajectory and process analysis, we quantify the main moisture sources and deeply explain the mechanisms of the significant precipitation interannual fluctuations observed in NWC.

2. Data and methods

In this study, we assess the wind field and water vapor simulation using the ERA5 reanalysis data obtained from the Copernicus Climate Change Service. The ERA5 dataset www.ecmwf.int/en/forecasts/datasets/reanalysis-datasets/era5, with a monthly temporal resolution and a spatial resolution of 0.25° × 0.25°, has been previously validated for its reliability in reproducing the historical water vapor distribution over Eurasia (Yao *et al* 2020). To account for the significant spatiotemporal variability of precipitation, we employed three precipitation datasets, which have been used by previous studies to evaluate model performance of precipitation in and around Eurasia (Ma *et al* 2009, Sun *et al* 2018). The first one is the Global Precipitation Climatology Project (GPCP) precipitation dataset www.ncei.noaa.gov/products/global-precipitation-climatology-project, provided by the NASA Global Precipitation Climatology Centre, which combines infrared and microwave data from multiple satellites and is corrected by data from various stations worldwide (Huffman *et al* 2013). This dataset covers the period from 1979 to the present, and has a horizontal resolution of 2.5° × 2.5°. Additionally, we employ the Climate Prediction Center Merged Analysis of Precipitation (CMAP) dataset https://psl.noaa.gov/data/gridded/data.cmap.html, a global monthly precipitation dataset created by the National Oceanic and Atmospheric Administration (NOAA) Climate Prediction Center. This dataset combines precipitation data from ground-based rain gauge observations, and has the same spatial resolution as that of GPCP. Finally, we use the NCEP reanalysis dataset www.weather.gov/ncep, which is a joint product of the National Centers for Environmental Prediction and the National Center for Atmospheric Research. This dataset combines observations and numerical weather prediction model outputs and has a spatial resolution of 1.875° × 1.875°.

In this study, we use the CAM5.1 global model to perform 40 years of simulation, with a horizontal resolution of 1.9° latitude by 2.5° longitude, covering the vertical range from the surface to 4 hPa through 56 layers (Hurrell *et al* 2013). To investigate the characteristics of moisture variability and its long-term trends, we use the MERRA2 meteorological field data required by the model to drive the model (Butler *et al* 2018, Tilmes *et al* 2022) and to obtain initial water vapor temperatures, wind fields, etc. The horizontal resolution of the MERRA2 data is consistent with that of the CAM5.1 simulations. Historical sea surface temperature (SST) data for a given month are obtained using monthly average SST information provided by the NOAA (Hurrell *et al* 2013). Furthermore, in order to obtain stable initial values of water vapor and precipitation marker concentrations, we get rid of the first year's (1981) simulation and explore the simulation results for the period of 1982–2021.

The Eulerian AWT algorithm is implemented in the CAM5.1. Firstly, the global domain is divided into several source regions (according to research needs), each containing five identified tracers for atmospheric moisture constituents (water vapor, cloud droplets, ice crystals, precipitation, and snow). Within each source region, the surface flux of the tagged moisture tracer (vapor) is equal to the surface evaporation flux from its own region, while it is zero outside the source region. These identified tracers for atmospheric moisture constituents undergo the same series of physical processes (deep convection, shallow

convection, cloud macrophysics, cloud microphysics, advection, and vertical diffusion) as the original atmospheric moisture constituents in the model, as detailed in Pan *et al* (2017). Finally, the contributions of atmospheric moisture constituents from a certain source area to any other locations are obtained from the simulation results. Therefore, the AWT method can quantitate moisture sources and their precipitation conversion rates globally (Jiang *et al* 2020, Pan *et al* 2023).

3. Results

3.1. Source region delineation

To investigate moisture sources over NWC, a global climate model (CAM5.1) was used, and the global surface was divided into 15 source regions (figure 1), with identifiers for the AWT (water vapor, cloud droplets, ice crystals, precipitation and snow) in each source region. The typical lifetime of water vapor in the atmosphere is about 7–10 d (Gimeno *et al* 2021). Some moisture may only be transported hundreds of kilometers, while other moisture can drift over millions of kilometers. Firstly, we divided the areas in more detail around the study region (NWC). NWC is defined based on its administrative boundaries (including Shaanxi, Gansu, Ningxia, Qinghai, and Xinjiang), covering the northern part of the Qinghai-Tibet Plateau. Building on prior research, the STP is an important moisture source and should be divided into a separate region (STP; Pan *et al* 2019). Southeast China significantly contributes to precipitation in NWC, leading to the further division of East Asia into Northeast Asia (NEA, northern) and Southeast China (SEC, southern; Huang *et al* 2015, Wu *et al* 2019). Secondly, external regions are classified by continents and oceans, such as Europe (EUP), Africa (AF), the North Indian Ocean (NIO), and the Northwest Pacific (NWP). Given that moisture rarely crosses hemispheres, regions like the Americas are grouped with other land areas (OLA), while the Southern Hemisphere oceans are designated as other marine areas (OMA).

3.2. Dominant summer moisture sources over NWC

The CAM5.1 simulation may overestimate tropospheric water vapor concentrations in certain regions, possibly influenced by strong convection and inadequate sensitivity to regional climatic features (such as monsoon), leading to increased uncertainty (Singh *et al* 2024). Despite these biases, it effectively captures the spatial distribution of water vapor columns and precipitation over Eurasia and adjacent regions, providing valuable results into moisture transport and transformation dynamics in NWC (Comparison results were shown in supplementary figures 1 and 2). Our study on interannual precipitation fluctuations in NWC indicates larger variability, indicating that CAM5 simulations are highly influenced by changes in convective activity and atmospheric circulation under climate change. However, these simulations align well with GPCP observational data (correlation coefficient of 0.85), suggesting the model effectively captures both low and high precipitation variations in NWC. Over a 40 year period, figures 3(a)–(d) showed monthly averaged absolute and relative contributions of various moisture source regions to vertical column-integrated water vapor (surface to top of atmosphere) and surface precipitation over NWC. During summer (JJA), local evaporation contributed 4.65 kg m^{-2} (21.3%) of water vapor and 0.37 mm d^{-1} (18.0%) of precipitation. The dominant terrestrial source regions were the NA, Europe (EUP), southern Qinghai-Tibet Plateau (STP) and SEC, contributing 4.18 kg m^{-2} (19.2%) of water vapor and 0.22 mm d^{-1} (11.2%) of precipitation, 3.61 kg m^{-2} (16.6%) and 0.23 mm d^{-1} (11.5%), 1.03 kg m^{-2} (4.7%) and 0.19 mm d^{-1} (9.5%), 0.97 kg m^{-2} (4.4%) and 0.17 mm d^{-1} (8.2%), respectively. These terrestrial sources collectively contributed 82% of water vapor and 77% of precipitation. Notably, the NIO contributed 1.39 kg m^{-2} (6.3%) of water vapor and 0.24 mm d^{-1} (11.5%) of precipitation, indicating efficient conversion of water vapor into precipitation, as further detailed in the following formula (1).

Interestingly, the contributions of water vapor and precipitation from different moisture sources to NWC exhibited obvious variations. For instance, precipitation ratios contributed to the NWC from the STP (9.5%) and SEC (8.2%) exceeded their respective water vapor ratios (4.7% and 4.4%), whereas the opposite was observed for NA (11.2% of precipitation, 19.2% of water vapor) and EUP (11.5% and 16.6%). Precipitation conversion efficiency E is defined as (Huang *et al* 1988, Wang *et al* 2019):

$$E_{i,\mathrm{NWC}} = \frac{P_i}{Q_i} * 100\%. \quad (1)$$

Here, P denotes surface precipitation (mm d^{-1}), Q represents the mass of water vapor in a column of air (kg m^{-2} d^{-1}), and the subscripts i denotes different source regions. As such, $E_{i,\mathrm{NWC}}$ indicates the precipitation efficiency of moisture from i region in NWC. We found higher precipitation conversion efficiencies for STP and SEC (southeasterly airflow transport; 19.1% and 17.6%) compared to EUP and NA (northwesterly airflow transport; 6.4% and 5.5%). Spatially, STP and SEC's contributions were concentrated in the southeastern NWC influenced by local topography and airflow convergence, thereby enhancing precipitation generation (supplementary figures 3(c) and (d)). In contrast, NA and EUP's contributions occurred in the western NWC under

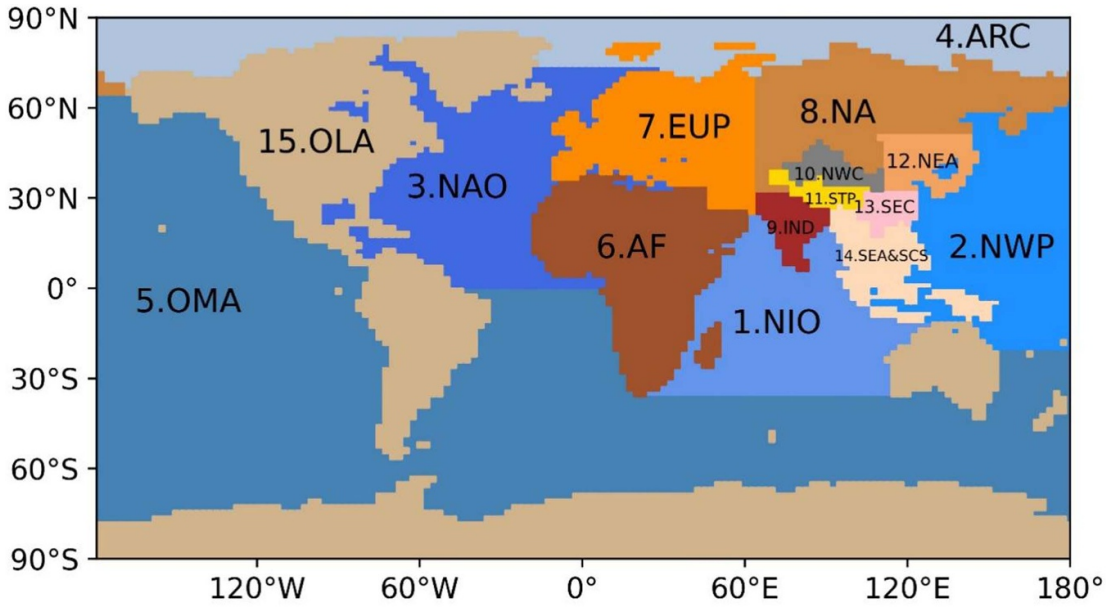

Figure 1. Fifteen moisture source regions tagged in this study: (1) North Indian Ocean (NIO); (2) Northwest Pacific Ocean (NWP); (3) North Atlantic Ocean (NAO); (4) Arctic Ocean (ARC); (5) Other Marine Areas (OMA); (6) Africa (AF); (7) Europe (EUP); (8) North Asia (NA); (9) India (IND); (10) Northwest China (NWC, including northern Qinghai-Tibet Plateau); (11) Southern Qinghai-Tibet Plateau (STP); (12) Northeast Asia (NEA); (13) Southeast China (SEC); (14) Southeast Asia and South China Sea (SEA&SCS); (15) Other Land Areas (OLA).

the influence of upper westerly jets and anticyclone, which typically suppressed precipitation (supplementary figures 3(a), (b) and 4).

3.3. General trend of summer precipitation over NWC

Previous studies have evaluated the reliability of GPCP data in capturing China's spatial and temporal precipitation variability (Ma *et al* 2009). Comparatively, the model used in this study demonstrated a satisfactory reproduction of interannual precipitation variability in the NWC, as indicated by a correlation coefficient of 0.85 (figure 2). From 1982 to 2021, summer precipitation in NWC has exhibited a notable increasing trend (1.6% in 40 years), particularly intensifying since 2000 (2.7% in 20 years), aligning with previous research results (Ren *et al* 2016, Li *et al* 2018).

As shown in table 1, the wetting trend was stronger in 2001–2021 than in 1982–2000. Next to the major increment from the local evaporation, the second major absolute increment (relative increment) was from the STP terrestrial source, with an annual average increment of 0.24 kg m^{-2} (26.7%, water vapor) and 0.05 mm d^{-1} (29.6%, precipitation), respectively. However, other terrestrial sources' increments (NA (0.12 kg m^{-2} and 0.02 mm d^{-1}), SEC (0.04 kg m^{-2} and 0.02 mm d^{-1}), EUP (−0.06 kg m^{-2} and 0.01 mm d^{-1})) and main oceanic sources (NIO (0.1 kg m^{-2} and 0.02 mm d^{-1}) and NWP (0.12 kg m^{-2} and 0.02 mm d^{-1})) were smaller in the 2 periods.

The above analyses suggest that the pronounced increase in water vapor and precipitation during NWC summer after 2001 could be primarily attributed to increases in local evaporation and external transport from terrestrial sources (mainly STP). This analysis explicitly quantified previous qualitative assessments (Wu *et al* 2019, Zhang *et al* 2019), offering a detailed understanding of the dominant moisture sources affecting NWC.

3.4. Attribution of summer precipitation fluctuations over NWC

Despite the recent wetting trend in NWC, there remain interannual fluctuations in precipitation (figure 2), manifesting as alternating dry and wet summers. Understanding moisture source differences and reasons during these periods is crucial. The normalized precipitation data was utilized to define dry and wet summers, effectively capturing interannual variations in precipitation intensity (Gutowski *et al* 2007). Standardized precipitation y over NWC was calculated using the formula (Wu *et al* 2001):

$$y = \frac{x - \bar{x}}{\sigma} \tag{2}$$

where x represented the annual average precipitation x (mm d^{-1}) from CAM5 simulation, $\bar{x}$ was the mean value of the 40 year average annual precipitation (mm d^{-1}), and σ was the standard deviation of the 40 year average annual precipitation (mm d^{-1}). The value of standardized precipitation y between −1

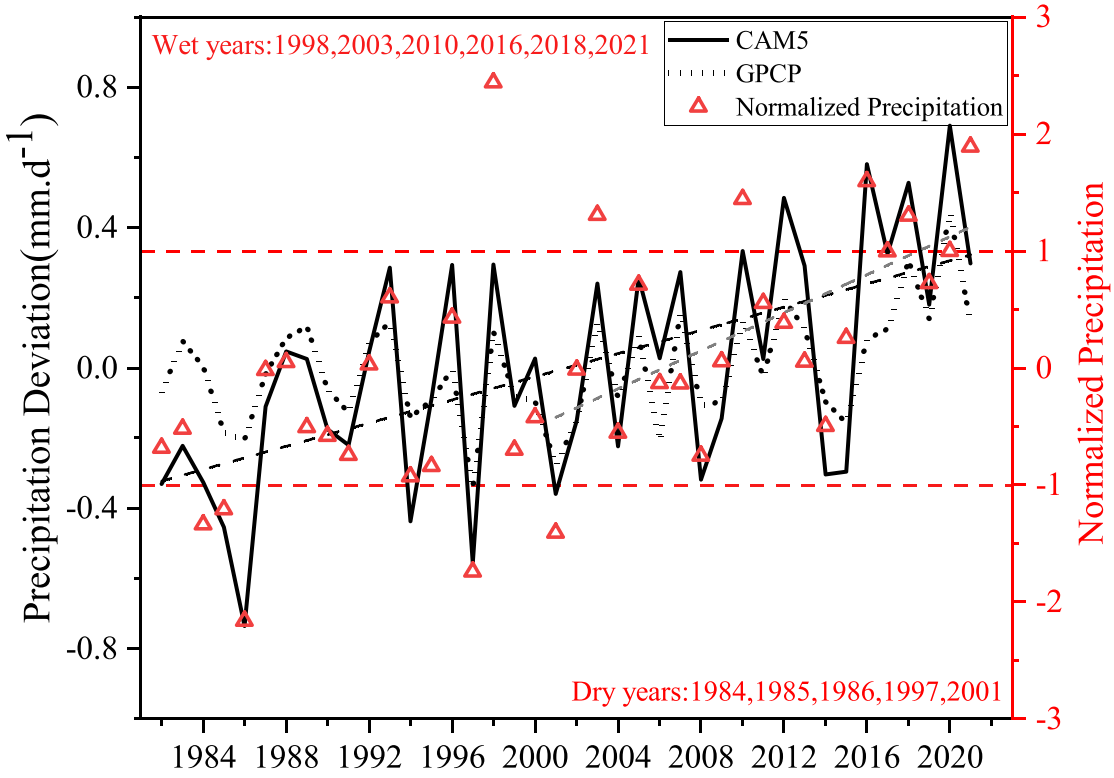

Figure 2. Interannual summer precipitation deviation of GPCP (dotted line) and simulated CAM5 (Solid line) in 1982–2021; normalized CAM5 summer precipitation (red triangle); line segment represents the growth rate of precipitation deviation (Black in 1982–2021, Grey in 2000–2021).

and 1 denoted a normal year, greater than 1 indicated a wet year, and less than −1 signified a dry year. Based on this standardized data (figure 2), wet years in NWC occurred notably in 1998, 2003, 2010, 2016, 2018, and 2021, whereas dry years were observed in 1984, 1985, 1986, 1997, and 2001.

Figure 4(a) depicts the moisture source contributions to precipitation over NWC during dry and wet summers. In wet summers, the local evapotranspiration contribution increased significantly, with absolute increments (wet summer contributions minus dry summers) and relative increments (The ratio of absolute increments to dry summers) of 0.18 mm d^{-1} and 69.8%, respectively. Among the terrestrial sources, the NA contributed the most increment with 0.13 mm d^{-1} (81.1%), followed by the STP with 0.08 mm d^{-1} (52.8%). As for oceanic sources (NIO and NWP), being distant from inland areas, encountered favorable weather systems and terrain uplifting during moisture transport. This process resulted in significant precipitation formation along the way of region (75° E–100° E, 0–25° N) to NWC from NIO, and region (125° E–135° E, 15° N–35° N) to NWC from NWP, and thus reducing direct oceanic moisture transport to the NWC (also shown as longitude and latitude moisture cross-sections in supplementary figures 5 and 6(a), (b)).

To validate the potential air masses contribution to increased summer precipitation in NWC, we analyzed 10 d back-trajectories (a semi-quantitative method) of all rainfall events in representative cities (northwestern part of NWC (Karamay) and southeastern part of NWC (Pingliang); shown in figure 5). Results indicate that during wet summers, enhanced precipitation in northwestern NWC was primarily influenced by intensified short-range northwesterly transport from NA, with a 16.7% relative increase. Nevertheless, in the southeastern NWC, increased precipitation was predominantly attributed to strengthened southeasterly transport from STP and NIO, which together increase by 21.1%. Therefore, both AWT and back-trajectory methods confirmed that terrestrial sources were the primary drivers of increased precipitation over NWC during wet summers, while the contribution from oceanic sources remained relatively stable.

Regarding the increased moisture transport from NA and STP to NWC, we found that while NA transported more moisture to NWC, its own precipitation did not increase significantly during NWC's wet summers (figure 4(b)). This was mainly because the weakened cyclonic systems prevailing in the northwestern NA (figure 6), resulted in reduced local precipitation efficiency (70° E–90° E, 50° N–60° N;

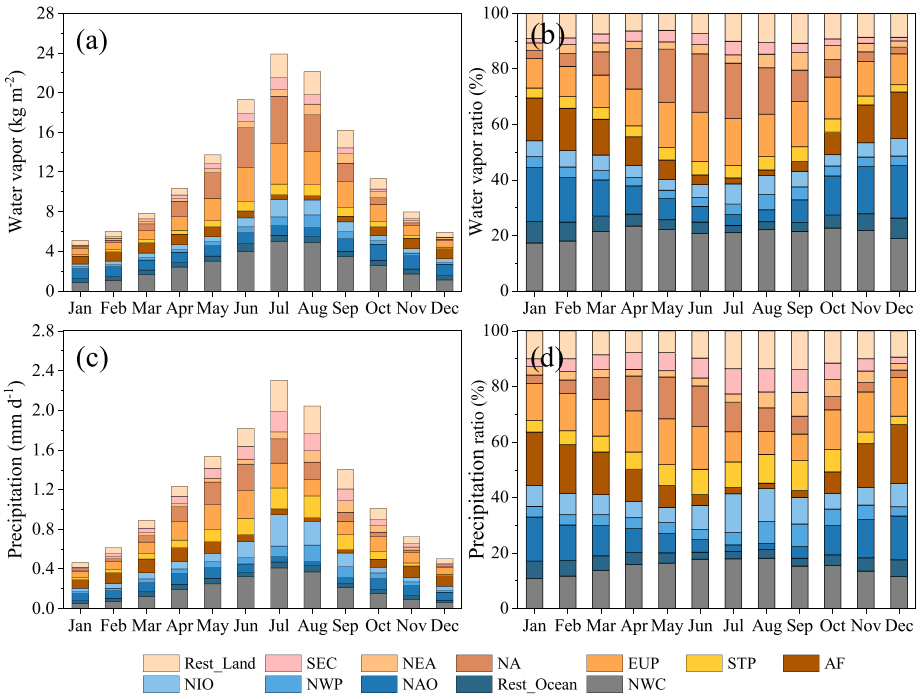

Figure 3. Monthly averaged (1982–2021) absolute contribution (a); (c) and percentage contribution (b); (d) of global moisture source regions to tropospheric water vapor content (a)–(b) and precipitation (c)–(d) over NWC (Rest_Land includes SEA, IND and OLA, Rest_Ocean includes ARC and OMA).

Table 1. The annual mean absolute (values outside the brackets, in kg m^{-2} of column water vapor and mm d^{-1} of precipitation) and relative (values inside the brackets, %) contributions from different moisture sources in NWC, and the absolute (relative) changes of column water vapor (precipitation) in NWC before and after 2000.

	NWC	STP	NA	SEC	EUP	NIO	NWP
				Water vapor (kg m^{-2})			
1982–2000	4.26 (20.5%)	0.90 (4.3%)	4.11 (19.8%)	0.94 (4.5%)	3.64 (17.5%)	1.33 (6.4%)	0.84 (4.1%)
2001–2021	5.01 (22.3%)	1.14 (5.1%)	4.23 (18.8%)	0.98 (4.4%)	3.58 (16.0%)	1.43 (6.4%)	0.96 (4.3%)
Absolute (Relative) increment from 2001–2021–1982–2000	0.75 (17.6%)	0.24 (26.7%)	0.12 (2.9%)	0.04 (4.3%)	−0.06 (−1.6%)	0.10 (7.5%)	0.12 (14.3%)
				Precipitation (mm d^{-1})			
1982–2000	0.33 (17.4%)	0.17 (8.9%)	0.22 (11.2%)	0.16 (8.5%)	0.23 (11.9%)	0.23 (12.2%)	0.10 (5.2%)
2001–2021	0.40 (18.4%)	0.22 (10.1%)	0.24 (10.9%)	0.18 (8.1%)	0.24 (10.9%)	0.25 (11.3%)	0.12 (5.5%)
Absolute (Relative) increment from 2001–2021–1982–2000	0.07 (20.4%)	0.05 (29.6%)	0.02 (11.0%)	0.02 (8.9%)	0.01 (4.2%)	0.02 (6.2%)	0.02 (20.4%)

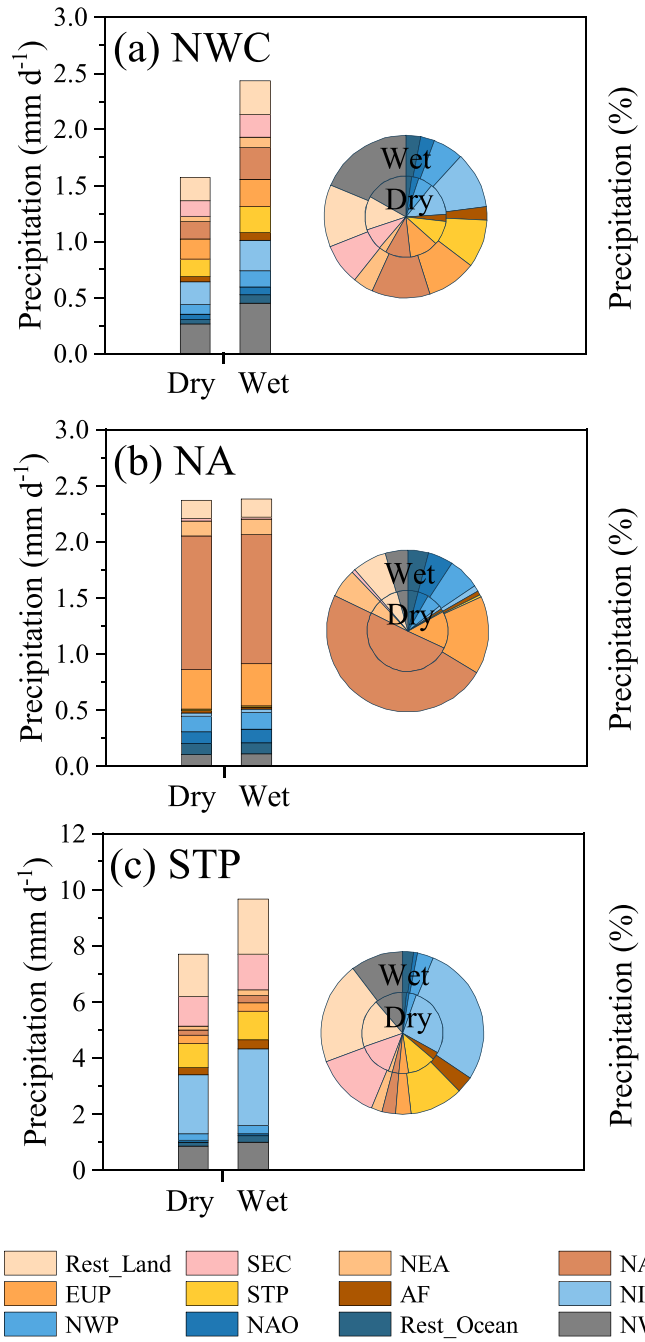

Figure 4. Average monthly absolute contributions (Bar charts) and percentage contributions (Pie charts) to NWC (a), NA (b) and STP (c) precipitation by global water source zones from dry to wet summers during 1982–2021.

supplementary figures 6(b), (f), (d) and (h)) and enhanced surface evaporation (supplementary figure 7). Subsequently, as the Iranian High Pressure moved eastward, residual moisture was transported to NWC, ultimately enhancing precipitation therein. Different to NA, the total precipitation over STP significantly increased, primarily due to moisture transported from NIO (0.62 mm d^{-1}; figure 4(c)). Building on the preceding discussion of moisture transport from NIO, it was initially deposited in the southern STP during transport, subsequently evaporated from STP (supplementary figure 7) and then was transported to the NWC.

3.5. Uncertainties

This study compares GPCP and CAM5.1 precipitation, alongside previous research (Pan *et al* 2017, Jiang *et al* 2020), demonstrating that CAM5.1 effectively reproduces the distributions of wind, water vapor and total precipitation. However, the model still exhibits some overestimations and underestimations, which may lead to biases in the

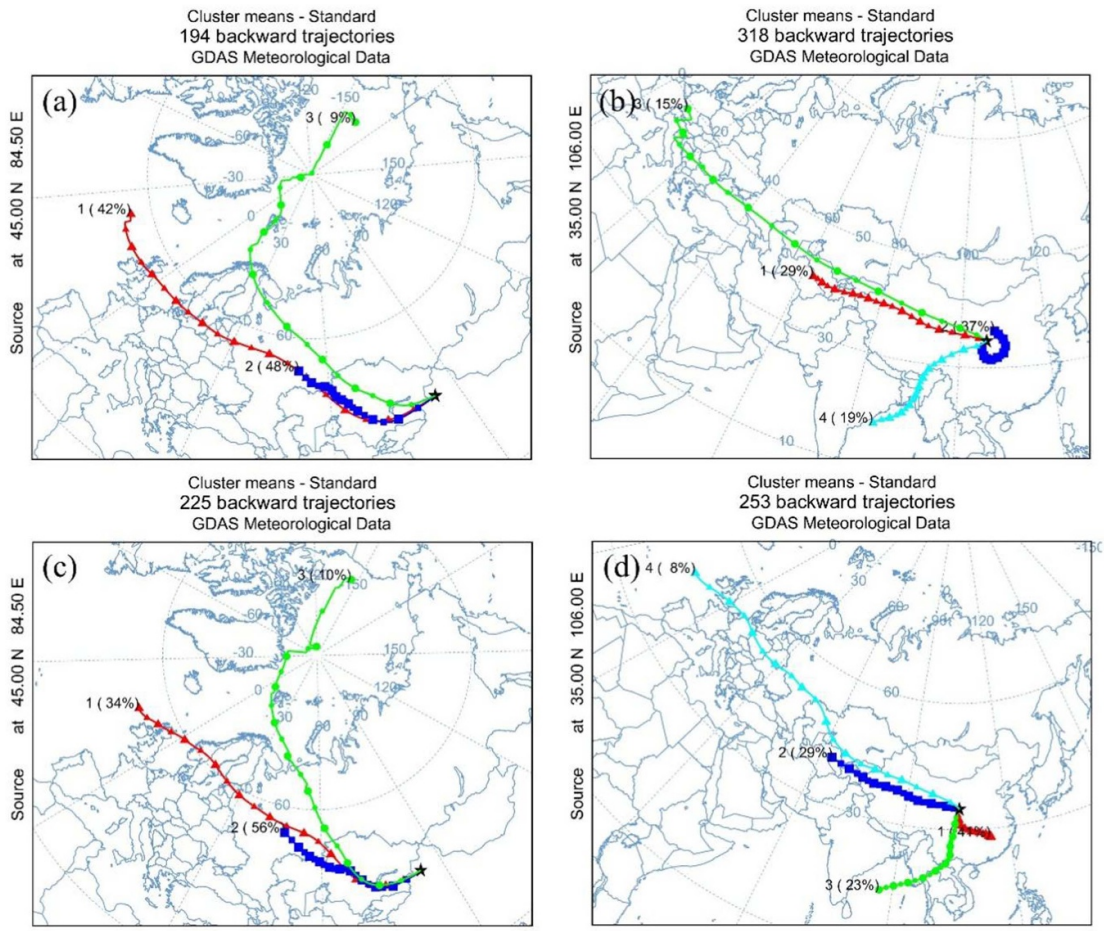

Figure 5. Cluster trajectory maps of moisture sources during precipitation events in dry (First line) and wet (Second line) summers in the typical regions (a), (c). Northwestern NWC (KLMY) & (b), (d). Southeastern NWC (PL)) of the NWC from 2005 to 2021 Based on HYSPLIT.

identified moisture sources and precipitation conversion rates in NWC. Additionally, the CAM5.1 tends to overestimate heavy rainfall events, reflecting ongoing challenges in differentiating convective and stratiform precipitation within current global climate models (Dai *et al* 2006). Therefore, further advancements in physical parameterization are essential for improving global climate models and enhancing the accuracy of AWT tracking results.

4. Conclusion and discussion

NWC, an inland region of China, has experienced a significantly wetting trend over the past 40 years, particularly intensifying after 2000. This change is attributed to an enhanced local evaporation (20.4% relative increase, i.e. 0.07 mm d^{-1} absolute increase) and increased external moisture influx from the STP (29.4%, 0.05 mm d^{-1}). Further investigation indicated that long-term water vapor and precipitation in NWC were closely linked to inputs from local evaporation and terrestrial sources, with NA, EUP, STP, and SEC identified as major contributors (collectively 82% of water vapor and 77% of precipitation), rather than oceanic sources. We also found that water vapor transported via southeasterly airflow (STP and SEC) to NWC more effectively induced precipitation under cyclonic systems, compared to northwesterly airflow (EUP and NA) over NWC, emphasizing the need to consider local synoptics more than mere moisture pathways (maybe 'pass-through moisture') in diagnosing moisture sources.

The upward wetting trend in NWC was also accompanied by interannual fluctuations in precipitation, manifesting as alternating dry and wet summers, primarily driven by increased moisture contributions from STP and NA (among dominant terrestrial sources). Specifically, the NA encountered the weakening of local cyclonic systems, thereby amplifying its evaporation and subsequent transport to NWC. While STP obtained increased precipitation and enhanced more moisture evaporation and transport to NWC due to the moisture from the NIO deposited in STP first during transport. These two distinct mechanisms underscore the complexity of terrestrial sources as moisture contributors.

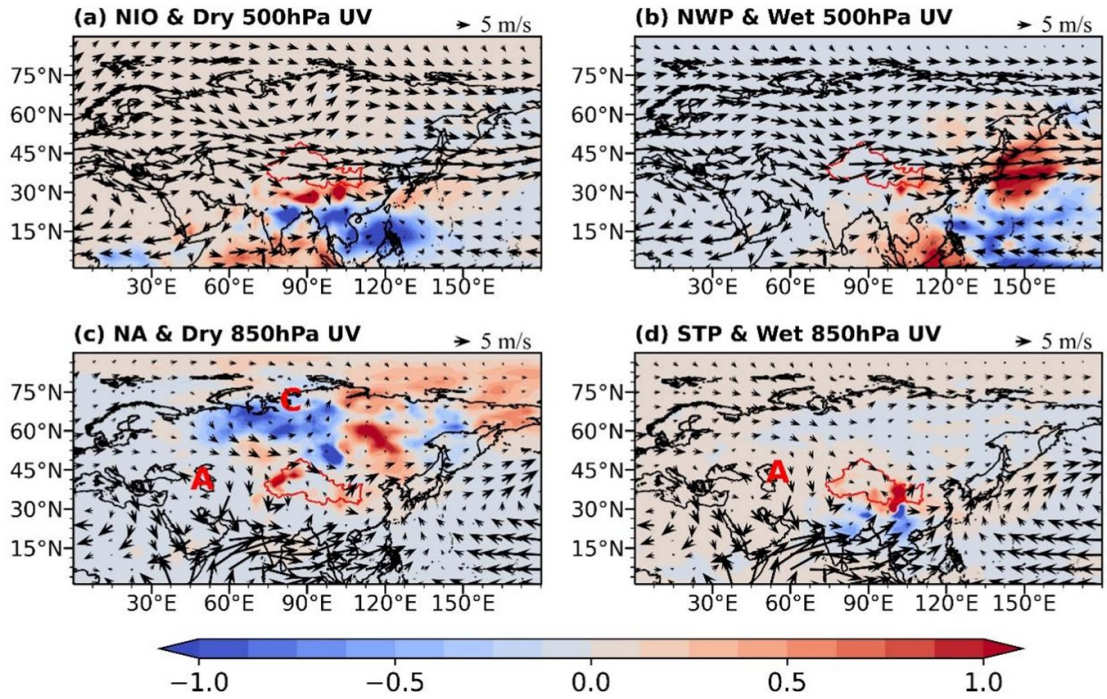

Figure 6. The differences of normalized precipitation (mm d^{-1}) between wet and dry summers originating from the sources of (a). NIO, (b). NWP, (c). NA, and (d). STP in Eurasia and surrounding areas (shaded) and the arrowed sections depict wind field maps at 500 hPa and 850 hPa for dry and wet summers.

This article enhances the understanding of moisture sources in NWC by clarifying the key roles of local evaporation and terrestrial inputs in wetting trends, while also highlighting the complex interactions between these moisture sources and atmospheric circulation systems that affect precipitation patterns.

Data availability statement

All data that support the findings of this study are included within the article (and any supplementary files).

Acknowledgment

This work is supported by Grants from the National Natural Science Foundation of China (Grant Nos. 42021004, 42175099).

Conflict of interest

The authors declare no competing interests.

Author contributions

Bin Zhu and Peng Qian conceived the study. Peng Qian and Bin Zhu designed the experiments. Peng Qian, Bin Zhu, Chunsong Lu, Haishan Chen and Hong Liao conducted the analysis. Peng Qian, Bin Zhu and Tong Zhu interpreted the results and jointly wrote and revised the paper. Peng Qian, Bin Zhu and Chenwei Fang provided the model runs. Hong Liao and Bin Zhu provided project funding.

ORCID iDs

Peng Qian https://orcid.org/0009-0005-8160-8337
Haishan Chen https://orcid.org/0000-0002-2403-3187

References

Bonne J L, Masson-Delmotte V, Cattani O, Delmotte M, Risi C, Sodemann H and Steen-Larsen H C 2014 The isotopic composition of water vapour and precipitation in Ivittuut, southern Greenland *Atmos. Chem. Phys.* **14** 4419–39

Butler T, Lupascu A, Coates J and Zhu S 2018 TOAST 1.0: tropospheric ozone attribution of sources with tagging for CESM 1.2.2 *Geosci. Model Dev.* **11** 2825–40

Dai A 2006 Precipitation characteristics in eighteen coupled climate models *J. Clim.* **19** 4605–30

Deng H X, Tang Q, Yun X, Tang Y, Liu X, Xu X, Sun S, Zhao G, Zhang Y and Zhang Y 2022 Wetting trend in Northwest China reversed by warmer temperature and drier air *J. Hydrol.* **613** 128435

Gao J, Jiao K and Wu S 2018 Quantitative assessment of ecosystem vulnerability to climate change: methodology and application in China *Environ. Res. Lett.* **13** 094016

Gimeno L, Eiras-Barca J, Durán-Quesada A M, Dominguez F, van der Ent R, Sodemann H, Sánchez-Murillo R, Nieto R and Kirchner J W 2021 The residence time of water vapour in the atmosphere *Nat. Rev. Earth Environ.* **2** 558–69

Gutowski W J, Takle E S, Kozak K A, Patton J C, Arritt R W and Christensen J H 2007 A possible constraint on regional

precipitation intensity changes under global warming *J. Hydrometeorol.* **8** 1382–96
Hu Q, Zhao Y, Huang A, Ma P and Ming J 2021 Moisture transport and sources of the extreme precipitation over Northern and Southern Xinjiang in the summer half-year during 1979–2018 *Front. Earth Sci.* **9** 770877
Huang M *et al* 1988 Effects of stratiform cloud on the development of cumulus cloud and its precipitation *J. Meteorol. Res.* **2** 215–22
Huang W, Feng S, Chen J and Chen F 2015 Physical mechanisms of summer precipitation V 318 ariations in the Tarim Basin in Northwestern China *J. Clim.* **28** 3579–91
Huffman G J and Bolvin D T 2013 Version 1.2 GPCP one-degree daily precipitation data set documentation (available at: https://rda.ucar.edu/datasets/ds728)
Hurrell J W *et al* 2013 The community Earth system model: a framework for collaborative research *Bull. Am. Meteorol. Soc.* **94** 1339–60
Jiang J, Zhou T, Wang H, Qian Y, Noone D and Man W 2020 Tracking moisture sources of precipitation over Central Asia: a study based on the water-source-tagging method *J. Clim.* **33** 10339–55
Li B F, Chen Y N and Shi X 2012 Why does the temperature rise faster in the arid region of Northwest China? *J. Geophys. Res. Atmos.* **117** D16115
Li B, Chen Y, Chen Z, Xiong H and Lian L 2016 Why does precipitation in Northwest China show a significant increasing trend from 1960 to 2010? *Atmos. Res.* **167** 275–84
Li C, Zwiers F, Zhang X, Li G, Sun Y and Wehner M 2021 Changes in annual extremes of daily temperature and precipitation in CMIP6 models *J. Clim.* **34** 3441–60
Li M and Ma Z 2018 Decadal changes in summer precipitation over arid Northwest China and associated atmospheric circulations *Int. J. Climatol.* **38** 4496–508
Lu S, Hu Z, Yu H, Fan W, Fu C and Wu D 2021 Changes of extreme precipitation and its associated mechanisms in Northwest China *Adv. Atmos. Sci.* **38** 1665–81
Ma L, Zhang T, Frauenfeld O W, Ye B, Yang D and Qin D 2009 Evaluation of precipitation from the ERA-40, NCEP-1, and NCEP-2 reanalyses and CMAP-1, CMAP-2, and GPCP-2 with ground-based measurements in China *J. Geophys. Res. Atmos.* **114** D9
Pan C *et al* 2023 The characteristics of the Yangtze flooding during 1998 and 2020 based on atmospheric water tracing *Geophys. Res. Lett.* **50** e2023GL104195
Pan C, Zhu B, Gao J and Kang H 2017 Source apportionment of atmospheric water over East Asia—a source tracer study in CAM5.1 *Geosci. Model Dev.* **10** 673–88
Pan C, Zhu B, Gao J, Kang H and Zhu T 2019 Quantitative identification of moisture sources over the Tibetan Plateau and the relationship between thermal forcing and moisture transport *Clim. Dyn.* **52** 181–96
Peng D and Zhou T 2017 Why was the arid and semiarid Northwest China getting wetter in the recent decades? *J. Geophys. Res. Atmos.* **122** 9060–75
Qian W, Fu J and Yan Z 2007 Decrease of light rain events in summer associated with a warming environment in China during 1961–2005 *Geophys. Res. Lett.* **34** 11
Qu L L, Yao J Q and Zhao Y 2023 Mechanism analysis of the summer dry-wet interdecadal transition in the Tarim Basin, Northwest China *Atmos. Res.* **291** 106840
Ren G Y *et al* 2016 Changes in precipitation over Northwest China *Arid Zone Res.* **33** 1–19 (in Chinese)
Shi Y F *et al* 2003 Discussion on the present climate change from warm-dry to warm wet in Northwest China *Quat. Res.* **23** 152–64 (in Chinese)
Singh B B, Krishnan R, Sabin T P, Vellore R K, Ganeshi N and Srivastava M K 2024 Upper tropospheric moistening during the Asian summer monsoon in a changing climate *Clim. Dyn.* **62** 55–68
Sun Q, Miao C, Duan Q, Ashouri H, Sorooshian S and Hsu K-L 2018 A review of global precipitation data sets: data sources, estimation, and intercomparisons *Rev. Geophys.* **56** 79–107
Tilmes S 2022 MERRA2 global forcing data for CESM2 applications (https://doi.org/10.5065/H9NM-XC59)
Wang J *et al* 2019 Interdecadal variability of summer precipitation efficiency in East Asia *Adv. Meteorol.* **2019** 3563024
Wang K L, Jiang H and Zhao H Y 2005 Atmospheric water vapor transport from westerly and monsoon over the Northwest China *Adv. Water Sci.* **16** 432–8 (in Chinese)
Wang Q and Zhai P 2022 CMIP6 projections of the "warming-wetting" trend in Northwest China and related extreme events based on observational constraints *J. Meteorol. Res.* **36** 239–50
Wu H, Hayes M J, Weiss A and Hu Q 2001 An evaluation of the standardized precipitation index, the China-Z index and the statistical Z-score *Int. J. Climatol.* **21** 745–58
Wu P, Ding Y H, Liu Y and Li X 2019 The characteristics of moisture recycling and its impact on regional precipitation against the background of climate warming over Northwest China *Int. J. Climatol.* **39** 5241–55
Wu P, Liu Y, Ding Y H, Li X and Wang J 2022 Modulation of sea surface temperature over the North Atlantic and Indian-Pacific warm pool on interdecadal change of summer precipitation over Northwest China *Int. J. Climatol.* **42** 8526–38
Yao B, Teng S, Lai R, Xu X, Yin Y, Shi C and Liu C 2020 Can atmospheric reanalyses (CRA and ERA5) represent cloud spatiotemporal characteristics? *Atmos. Res.* **244** 105091
Zhang Q, Hu Y Q, Cao X Y and Liu W M 2000 About some problems of arid climate system of Northwest China *J. Desert Res.* **20** 357–62 (in Chinese)
Zhang Q, Lin J, Liu W and Han L 2019 Precipitation seesaw phenomenon and its formation mechanism in the eastern and western parts of Northwest China during flood season *Sci. China Earth Sci.* **62** 2083–98
Zhang Q, Yang J, Duan X, Ma P, Lu G, Zhu B, Liu X, Yue P, Wang Y and Liu W 2022 The eastward expansion of the climate humidification trend in Northwest China and the synergistic influences on the circulation mechanism *Clim. Dyn.* **59** 2481–97
Zhang Q, Zhu B, Yang J, Ma P, Liu X, Lu G, Wang Y, Yu H, Liu W and Wang D 2021 New characteristics about the climate humidification trend in Northwest China *Chin. Sci. Bull.* **66** 3757–71
Zhang Y H and Wu Y Q 2007 Variation of $\delta^{18}O$ in water in Heihe river basin *Adv. Water Sci.* **18** 864–70 (in Chinese)